

The resulting dimensionless velocity profiles for both pseudoplastic and dilatant fluids are plotted in Figure 1 for the case  $\Omega = 1/3$ . For increasing values of the rheological exponent  $n$  the effective width of the momentum mixing region decreases, but the approach to the final steady state [in which the velocity is everywhere equal to  $1/2 (U_1 + U_2)$ ] becomes slower as  $n$  increases. For  $n > 1$ , the velocity profiles approach a linear profile as  $n$  increases, a behavior common to steady dilatant flows in pipes and channels.

#### ACKNOWLEDGMENT

This research was supported by the Advanced Research Projects Agency (Project DEFENDER) under Contract No. DA-31-124-ARO-D-257, monitored by the U.S. Army Research Office-Durham.

#### NOTATION

$B_n$  = constant of integration  
 $f$  = dimensionless velocity distribution

$m, n$  = parameters characterizing a power law fluid  
 $t$  = time after mixing begins  
 $u$  = fluid velocity  
 $U_1$  = initial velocity of upper stream  
 $U_2$  = initial velocity of lower stream  
 $V$  = initial velocity difference between two streams  
 $y$  = distance from centerline

#### Greek Letters

$\Gamma$  = gamma function  
 $\zeta$  = dimensionless similarity variable  
 $\rho$  = fluid density  
 $\varphi_n$  = dimensionless velocity distribution as defined in reference 1  
 $\Omega$  =  $U_2/U_1$  = ratio of initial stream velocities

#### LITERATURE CITED

1. Bird, R. B., *A.I.Ch.E. J.*, **5**, 565 (1959).
2. Acrivos, A., M. J. Shah, and E. E. Petersen, *ibid.*, **6**, 312 (1960).

## On the Stability of a Continuous Flow Stirred-Tank Reactor

DAVID S. SABO and JOSHUA S. DRANOFF

Northwestern University, Evanston, Illinois

The stability of a self-regulating continuous flow stirred-tank reactor (CFSTR) has received considerable attention in recent years. Bilous and Amundson (1) presented the first detailed analysis for the case of an exothermic first-order reaction. They demonstrated the multiplicity of possible steady states and analyzed the stability of such states by means of linearization techniques. Berger and Perlmutter (2, 3) later applied Lyapunov's second method to obtain a conservative estimate of the region of asymptotic stability for the same problem. Most recently, Paradis and Perlmutter (4) used a tracking function technique to determine regions of practical stability and ultimate boundedness. The following development presents a scheme for the simple determination of a general region of ultimate boundedness as well as a set of natural tracking functions for such a system. Application to the special case of an adiabatic reactor system is also demonstrated.

The energy and material balance equations for a CFSTR equipped with a cooling jacket (or coil) are

$$\rho V C_p \frac{dT}{d\theta} = (-\Delta H) V k_o C e^{-E/RT} - A_r U (T - T_c) - \rho q C_p (T - T_o) \quad (1)$$

$$V \frac{dC}{d\theta} = -V k_o C e^{-E/RT} - q (C - C_o) \quad (2)$$

These equations assume first-order, irreversible reaction, constant coolant temperature, and constant physical properties. For convenience, dimensionless variables may be defined and the equations rewritten as follows. Let

$$\bar{T} = T / \left[ \frac{U A_r T_c}{\rho q C_p} + T_o \right] \quad (3)$$

$$\bar{C} = C/C_o \quad (4)$$

$$\bar{\theta} = \theta q/V \quad (5)$$

Then

$$d\bar{T}/d\bar{\theta} = \alpha \beta \bar{C} e^{-\delta/\bar{T}} - \gamma \bar{T} + 1 \quad (6)$$

and

$$d\bar{C}/d\bar{\theta} = -\alpha \bar{C} e^{-\delta/\bar{T}} - \bar{C} + 1 \quad (7)$$

where

$$\alpha = k_o V/q \quad (8)$$

$$\beta = (-\Delta H) C_o / \left[ \rho C_p \left\{ \frac{U A_r T_c}{\rho q C_p} + T_o \right\} \right] \quad (9)$$

$$\gamma = \frac{U A_r}{\rho q C_p} + 1 \quad (10)$$

$$\delta = \left[ \frac{E}{R} \frac{1}{\left( \frac{U A_r T_c}{\rho q C_p} + T_o \right)} \right] \quad (11)$$

Now, if Equation (7) is multiplied by  $\beta$  and added to Equation (6), one obtains

$$\frac{d(\bar{T} + \beta \bar{C})}{d\bar{\theta}} = -[(\gamma \bar{T} + \beta \bar{C}) - (1 + \beta)] \quad (12)$$

This equation provides the key to further analysis. When the reactor system is at steady state, the left-hand side of Equation (12) is equal to zero, so that the steady state (or singular) points of Equations (6) and (7) must lie on a straight line—the steady state line—given by

$$\gamma \bar{T} + \beta \bar{C} = 1 + \beta \quad (13)$$

Figure 1 shows a phase plane with this readily determined steady state locus indicated as a dotted line. Also shown are contours of constant  $(\bar{T} + \beta \bar{C})$ . All of these lines

may be easily sketched when the values of  $\beta$  and  $\gamma$  are specified.

The dynamic progress of the system from any starting point to steady state may be shown as a trajectory on this phase plane plot. According to Equation (12), any trajectory starting from a point above the steady state line, on the contour  $(\bar{T} + \beta\bar{C}) = K_2$ , for example, will move in the direction of decreasing  $(\bar{T} + \beta\bar{C})$ , since the right side of the equation will be negative. In assuming that the trajectory does not go directly to a steady state point, it will cross the steady state line with  $(\bar{T} + \beta\bar{C})$  greater than  $\frac{1+\beta}{\gamma}$  as shown in Figure 1. Below the steady state line this trajectory will then move in the direction of increasing  $(\bar{T} + \beta\bar{C})$  according to Equation (12). Thus,  $(\bar{T} + \beta\bar{C})$  will remain greater than  $\frac{1+\beta}{\gamma}$ .

Similarly, any trajectory starting from a point below the steady state line, on the contour  $(\bar{T} + \beta\bar{C}) = K_1$  for example, will move toward larger values of  $(\bar{T} + \beta\bar{C})$  until it crosses the steady state line, at which point  $(\bar{T} + \beta\bar{C})$  will be less than  $(1 + \beta)$ . At this point the trajectory will move toward lower values of  $(\bar{T} + \beta\bar{C})$  and thus  $\bar{T} + \beta\bar{C}$  will remain less than  $(1 + \beta)$ .

Therefore, it can be seen that all trajectories will enter and thereafter remain within a limited domain defined by the inequalities

$$\frac{1+\beta}{\gamma} \leq \bar{T} + \beta\bar{C} \leq 1 + \beta \quad (14)$$

The corresponding region is shown as the shaded area in Figure 1. This domain is, in the notation of Paradis and Perlmuter (4), a region of ultimate boundedness, since every trajectory of the system will eventually enter and remain within this region for times greater than some  $\tau > 0$ . It is not possible at this point to indicate the behavior of the system once a trajectory enters this domain without additional calculations. Thus, although asymptotic passage to the steady state point is expected, the possibility of limit cycle behavior cannot be dismissed, but is limited to the region of ultimate boundedness.

Paradis and Perlmuter have indicated how one may determine regions of practical stability and ultimate bound-

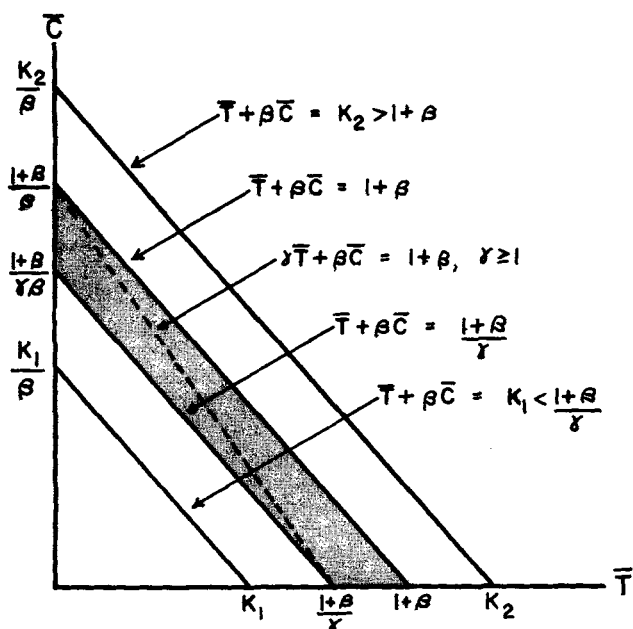


Fig. 1. Phase plane for single-step reaction.

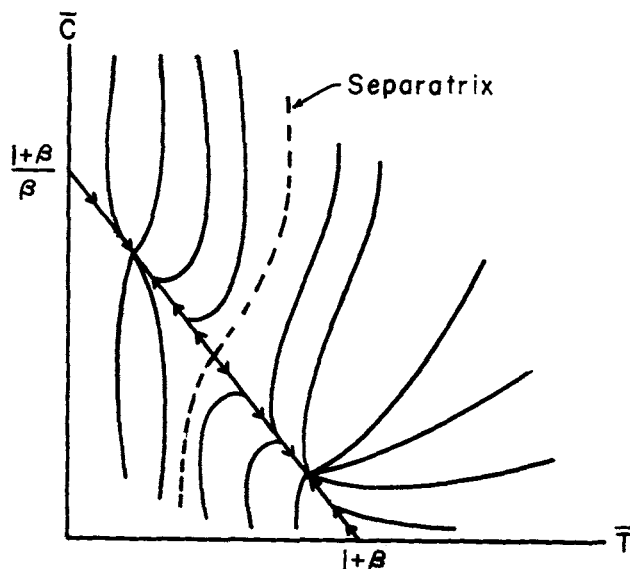


Fig. 2. Phase plane for adiabatic system with three steady states.

edness by calculations which involve simple tracking functions selected by trial and error methods. Equation (12) suggests that one set of reasonable candidates for such functions may be the contours of constant  $(\bar{T} + \beta\bar{C})$ . As described above, the dynamic behavior of the system can be easily sketched relative to such contours and the steady state locus of Equation (13).

Equation (12) can be exploited further for an adiabatic system. In this case  $\gamma = 1$  and Equation (12) is separable and directly solvable. The solution is

$$\bar{T} + \beta\bar{C} = 1 + \beta + [(\bar{T}_i + \beta\bar{C}_i) - (1 + \beta)] e^{-\theta} \quad (15)$$

where  $\bar{T}_i$  and  $\bar{C}_i$  correspond to an arbitrary starting point. The equation predicts that every trajectory will move monotonically to the steady state line, which in this case is a contour of  $\bar{T} + \beta\bar{C}$

$$\bar{T} + \beta\bar{C} = 1 + \beta \quad (16)$$

Once on this locus, the trajectories will move to the stable steady state points where they will terminate, as shown in Figure 2 for a system with two stable steady states. Limit cycles are clearly excluded in this case, while the region of ultimate boundedness is reduced to just the stable steady state points.

The phase plane now consists of two regions of asymptotic stability, corresponding to the two stable steady states, with a separatrix which passes through the unstable steady state. The stability analysis of the adiabatic case could be completed if one could analytically describe the separatrix, a task which thus far has proved impossible.

The foregoing has sought to show how the system equations for a self-regulating CFSTR can be quite simply manipulated to permit rapid determination of the steady state locus, a region of ultimate boundedness and a set of natural tracking functions. It is hoped that this approach may serve to provide additional insight into the stability of such a system.

#### NOTATION

- $A_r$  = reactor heat transfer area
- $C$  = reactant concentration
- $\bar{C}$  = dimensionless concentration, see Equation (4)
- $C_i$  = initial dimensionless concentration
- $C_o$  = inlet concentration
- $C_p$  = specific heat of reactor contents

$E$  = activation energy  
 $(-\Delta H)$  = exothermic heat of reaction  
 $k_o$  = frequency factor  
 $q$  = volumetric flow rate  
 $R$  = gas constant  
 $T$  = temperature  
 $\bar{T}$  = dimensionless temperature, see Equation (3)  
 $T_c$  = coolant temperature  
 $T_i$  = initial dimensionless temperature  
 $T_o$  = inlet temperature  
 $U$  = overall heat transfer coefficient  
 $V$  = reactor volume

#### Greek Letters

$\alpha$  see Equation (8)

$\beta$  see Equation (9)  
 $\gamma$  see Equation (10)  
 $\delta$  see Equation (11)  
 $\rho$  = density of reactor contents  
 $\theta$  = time  
 $\bar{\theta}$  = dimensionless time, see Equation (5)

#### LITERATURE CITED

1. Bilous, Oleg, and N. R. Amundson, *A.I.Ch.E. J.*, **1**, 513 (1955).
2. Berger, J. S., and D. D. Perlmutter, *ibid.*, **10**, 233 (1964).
3. ———, *Chem. Eng. Sci.*, **20**, 147 (1965).
4. Paradis, W. O., and D. D. Perlmutter, *A.I.Ch.E. J.*, **12**, 130 (1966).

## Effective Dispersion in a Tubular Flow Reactor with Return Bends

ALBERT GOMEZPLATA and CHAN M. PARK

University of Maryland, College Park, Maryland

The characterization of nonideal flow conditions in chemical reactors has received considerable attention recently, and is a logical step to be taken toward the realization of a closer design of chemical reactors. In the case of tubular reactors, or those that approach plug flow conditions, the use of a dispersion coefficient to take into account local mixing, as well as radial velocity variations, seems to be practical (3, 4). In the case of reactors with configurations that disrupt or bypass the flow, the use of mixed models has been proposed (3, 4). Bischoff (1) recently worked with a mixed model to obtain an effective dispersion coefficient from the data of Carter and Bir (2) on axial mixing in a tubular reactor with a number of return bends. He considered the straight sections as plug flow sections with axial mixing, and the return bends as perfect mixers. The representation of the return bends as completely mixed sections gives effective dispersion coefficients that fit the experimental data better than if the bends are ignored. A better fit might be expected if the return bends are considered as sections of greater axial mixing than the straight sections, but not as perfect mixers. We would like to illustrate this point by the use of a dispersion model where the dispersion coefficient for the return bends is a function of the dispersion coefficient in the straight sections and Reynolds number. The effective dispersion can then be made to exhibit a minimum as the Reynolds number is increased.

#### MODEL

Suppose we consider the dispersion coefficient at the bend section as some multiple of the dispersion coefficient in a straight pipe, that is

$$D_b = m D_p \quad (1)$$

This implies that the dispersion group at the bend section

is

$$\frac{D_b}{v L_{\text{beq}}} = m \frac{D_p}{v L_{\text{beq}}} \quad (2)$$

where  $L_{\text{beq}}$  is an equivalent length of the bend section. Then in a treatment similar to Bischoff's (1), the first and second moments for the straight sections are

$$\Delta\mu_{1p} = \left( \frac{L_p}{L} \right) \quad (3)$$

$$\Delta\sigma_p^2 = 2 \frac{D_p}{v L_p} \left( \frac{L_p}{L} \right)^2 \quad (4)$$

for the bend sections

$$\Delta\mu_{1b} = \left( \frac{L_{\text{beq}}}{L} \right) \quad (5)$$

$$\Delta\sigma_b^2 = m^2 \Delta\sigma_{p\text{eq}}^2 = m^2 \left( 2 \frac{D_p}{v L_{\text{beq}}} \right) \left( \frac{L_{\text{beq}}}{L} \right)^2 \quad (6)$$

and for the overall system

$$\Delta\mu_1 = 1 \quad (7)$$

$$\Delta\sigma^2 = 2 \left( \frac{D_e}{v L} \right) \quad (8)$$

From Equations (4), (6), and (8)

$$\frac{D_e}{v L} = \frac{D_p}{v L} \left( \frac{L_p}{L} \right) + m^2 \frac{D_p}{v L} \left( \frac{L_{\text{beq}}}{L} \right) \quad (9)$$

But from Equations (3), (5), and (7)

$$\frac{L_p}{L} = 1 - \left( \frac{L_{\text{beq}}}{L} \right) \quad (10)$$